

Near-Nuclei Magnetic Resonance of  $\text{CaF}_2:\text{Yb}^{3+}$ 

J. P. Wolfe and R. S. Markiewicz

Department of Physics, University of California, Berkeley, California 94720

(Received 9 April 1973)

We have observed discrete resonances for fluorine nuclei near  $\text{Yb}^{3+}$  impurities in  $\text{CaF}_2$ . Angular dependences are reported and some general features of the near-nuclei magnetic-resonance method are briefly discussed.

Local magnetic fields of paramagnetic impurities in crystals are known to shift the resonant fields of nearby nuclei away from the usual bulk NMR. At low temperatures, the impurity moment is effectively static and the resultant shifts can be several kilogauss. The splittings are derived from the spin Hamiltonian  $H = \beta \vec{S} \cdot \vec{g} \cdot \vec{H} + g_n \beta \vec{H} \cdot \vec{I} + \vec{S} \cdot \vec{A} \cdot \vec{I}$ , involving electron and nuclear Zeeman terms and the hyperfine interaction  $A = (A_{ij})$ . Using a high-sensitivity NMR spectrometer,<sup>1</sup> we have been able to detect directly these weak impurity-shifted resonances of fluorine nuclei near  $\text{Yb}^{3+}$  ions in calcium fluoride and thereby study the electron-nuclear interactions as well as lattice distortions associated with local charge compensation. Within the past decade, extensive electron-nuclear double-resonance (ENDOR) studies of rare-earth-doped  $\text{CaF}_2$  have provided detailed information about the electron-nuclear interactions, the nature of local charge compensation, and accompanying lattice distortions.<sup>2-5</sup> The interaction between the ion and second-shell fluorine is largely point-dipolar in form and magnitude; however, there are large covalent contributions to the first-shell interaction, and the Hamiltonian is usually characterized by the most general  $A$  matrix allowed by the symmetry. For a tetragonal  $\text{Yb}^{3+}$  site, arising from local charge compensation (Fig. 1), the  $C_{1h}$  point symmetry of a nearest-neighbor fluorine reduces the  $A$  matrix to five independent elements. The basic simplicity of the NMR technique lends itself to precise angular and field dependences of the near-fluorine resonances not previously obtained, allowing us to probe the form of the interaction. Initially, we have attempted to compare empirically the five-parameter form with a more intuitive (three-parameter) dipole-plus-scalar form  $A_{ij} = (3l_i l_j - \delta_{ij}) \times g_i A_p + \delta_{ij} A_s$ , where  $g_x = g_y = g_{\perp}$ ,  $g_z = g_{\parallel}$ , and  $l_i$  are the direction cosines from the rare earth to the near-neighbor fluorine. For the tetragonal symmetry,  $l_x = l_y$  and the three parameters are  $A_p$ ,  $A_s$ , and  $\mu = l_z/l_x$ . From the simple interpre-

tation of the three parameters, we have, for the first time, an indication of the first-shell distortion, Fig. 1. Our results for the first-shell and interstitial fluorine are described below.

*Cubic near neighbors.*—In the case of distant charge compensation, cubic symmetry is preserved, leading to the above  $A$  matrix with  $\mu=1$  and  $g_i = g_c$ . (The nearest-fluorine point symmetry is  $C_{3v}$ , reducing  $A$  to two independent parameters,  $A_p$  and  $A_s$ .)<sup>2</sup> The splittings of the cubic resonances in the (100) plane fit this interaction to within  $\delta H_{\text{rms}} = 8.1$  Oe over the entire 5-kOe range, Fig. 2(b). The data can be fitted with  $\delta H_{\text{rms}} = 2.3$  Oe by assuming additional small corrections proportional to the external magnetic field, partially arising from a second-order Zeeman effect among the  $\text{Yb}^{3+}$  crystal field levels. We have determined for the first time the absolute signs of  $A_s$  and  $A_p$ .<sup>6</sup> The signs are both positive; thus,  $A_p$  has the same sign as would be expected for a pure point-dipolar interaction,  $A_d = +2.43$  kOe, between the  $\text{Yb}^{3+}$  ion and the nearest-neighbor fluorine nuclei. Unlike ENDOR, there is no ambiguity in determining the sign of these parameters since the  $S_z = +\frac{1}{2}$  state is less intense than the  $S_z = -\frac{1}{2}$  state by the electronic

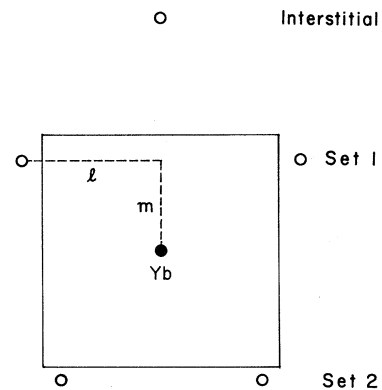


FIG. 1. Distortions of the first-shell fluorine atoms derived from the three-parameter fit. Our data and analysis yield  $\mu = m/l$  given in Table I, but the actual Yb-F distances are unknown.

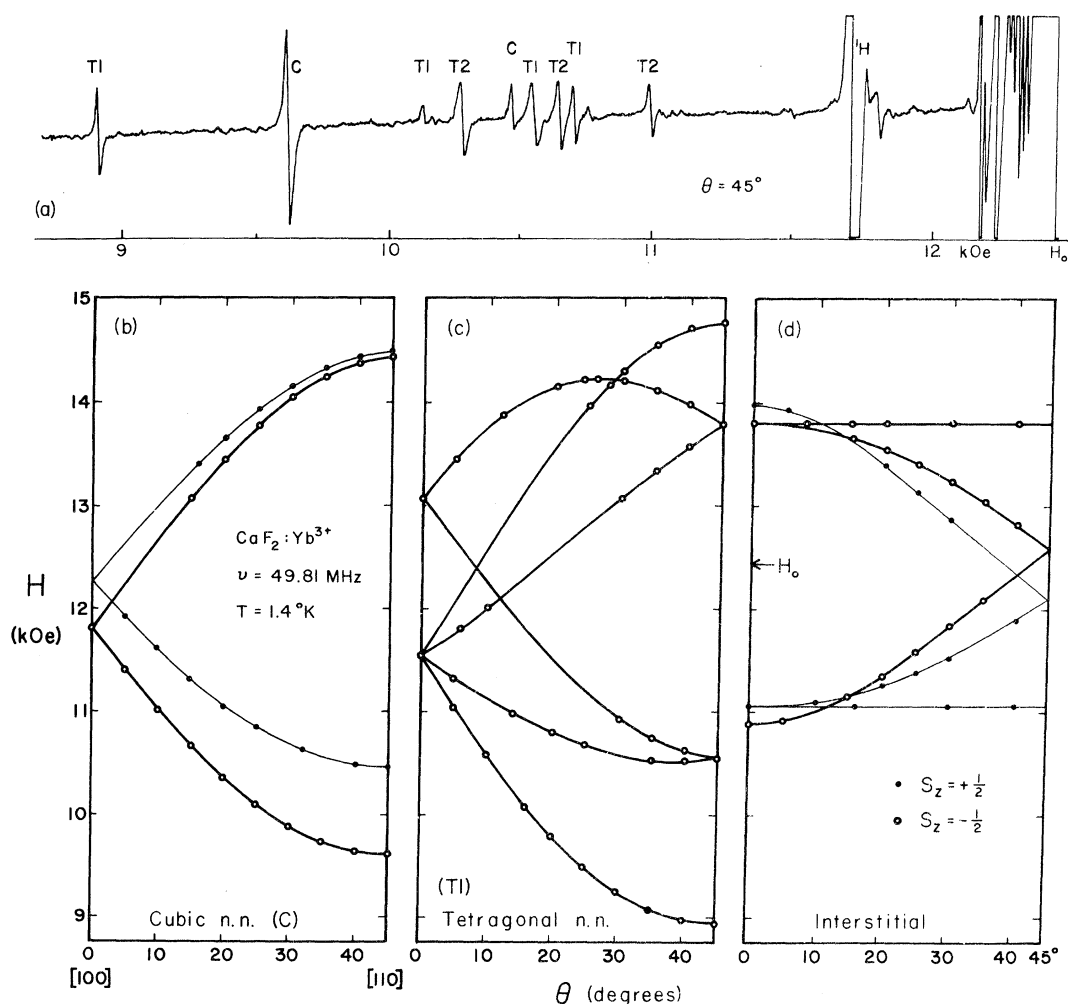


FIG. 2. (a) Near-fluorine spectrum. The bulk  $^{19}\text{F}$  resonance at  $H_0$  is  $10^4$  times off scale. (b), (c), (d) Angular dependences as  $H$  is rotated in (100) plane. Only  $S_z = -\frac{1}{2}$  branches of set 1 tetragonal near neighbors are shown. Parameters for the least-squares fits (solid curves) are given in Table I.

Boltzmann factor.

*Tetragonal near neighbors.*—The most striking feature of these angular dependences, Fig. 2(c), is the maximizing of certain branches away from the crystal axes, largely resulting from distortion of the first shell by the interstitial charge-compensating fluorine. The two sets of near neighbors each fit with  $\delta H_{\text{rms}} = 12$  Oe with the general, five-parameter interaction. (Experimental error is  $\pm 5$  Oe.) For the fluorines nearer the interstitial (set 1), the resulting three-parameter fit yielded  $\delta H_{\text{rms}} = 18$  Oe. For set 2, the three-parameter fit was somewhat worse, yet the maximum deviation was only 3% of the total splitting. Results are shown in Table I. Our least-squares fit simultaneously includes all branches and  $S_z = \pm \frac{1}{2}$  spin states. It is appar-

ent from this curve fitting, Fig. 2(c), that the scalar-plus-dipolar interaction gives fairly close agreement with the data, although deviations are not negligible. It is notable that the signs of the  $A_s$  parameters in this analysis are different for the two sets of fluorine nuclei. This is of considerable interest since the sign of  $A_s$  provides an important clue as to the origin of the covalency.<sup>7</sup>

*Tetragonal interstitial.*—The hyperfine parameters  $A_{\parallel} = 12.35$  and  $A_{\perp} = -10.97$  MHz derived from our angular data differ significantly from the values  $A_{\parallel} = 12.39$  and  $A_{\perp} = -8.70$  MHz measured by ENDOR.<sup>4</sup> The splittings for  $H$  along the [100] axis are found to be quite insensitive to field, as expected, from  $H_0 = 5$  to 15 kOe, lending further support to our assignments. Again

TABLE I. Fitted scalar and dipolar parameters for first-shell and interstitial fluorine in  $\text{CaF}_2:\text{Yb}^{3+}$ . The near-neighbor positions are defined by  $(l, l, m)$  with the interstitial at  $(0, 0, 2)$ , and  $\mu \equiv m/l$ . We have used  $g_c = 3.443$ ,  $g_{\parallel} = 2.412$ ,  $g_{\perp} = 3.802$  (Ref. 8). For the cubic case,  $g_c A_p$  ( $= 17.62$  MHz) is equivalent to  $A_p$  defined in Ref. 2.

Type of site	Absolute				
	Conc. (%)	$A_s$ [kOe (MHz)]	$A_p$ [kOe (MHz)]	$\mu$	$\delta H_{\text{Tms}}$ (Oe)
Cubic	0.009	0.449 (1.80)	1.278 (5.119)	(1.0)	8.1
Tetragonal Set 1	0.009	-0.139 (-0.557)	1.189 (4.763)	0.66	17.4
Set 2		0.575 (2.303)	1.018 (4.078)	1.31	54.1
Interstitial		-0.173 (-0.693)	0.675 (2.704)	...	13.2

the near-nuclei magnetic-resonance (NNMR) spectrum allows us to distinguish between  $S_z = \pm \frac{1}{2}$  branches, thereby fixing the absolute signs of  $A_{\parallel}$  and  $A_{\perp}$ , and hence the values of  $A_s$  and  $A_p$  from  $A_{\parallel} = A_s + 2g_{\parallel}A_p$  and  $A_{\perp} = A_s - g_{\perp}A_p$ .

In this  $\text{CaF}_2:\text{Yb}^{3+}$  crystal (nominal 0.05% from Optovac Company) we have also observed weaker resonances from trigonal sites. An obvious complication of this technique is that resonances from all of the above-mentioned sites are superimposed on the same field sweep; however, identification is greatly simplified by a comparison of relative intensities and saturation behavior. As a bonus, the ratio of integrated intensities for near and bulk resonances gives the absolute concentration of the various rare-earth sites in the crystal (determined within a factor of 2). As expected, the NNMR spectrum is quite insensitive to the nuclear spin of the impurity and to cross relaxation effects which complicate the ENDOR technique. Also, the method is applicable even where the EPR is weak or unobservable<sup>1</sup>; in particular, we have observed NNMR resonances for non-Kramers ions in  $\text{CaF}_2$ . In addition, observation of the near-nuclei resonances provides a point of departure for the study of nu-

clear relaxation on a microscopic scale. Our preliminary investigations on  $\text{CaF}_2$  indicate the broad flexibility of the NNMR method.

†Research supported in part by the U.S. Atomic Energy Commission.

<sup>1</sup>A. R. King, J. P. Wolfe, and R. L. Ballard, *Phys. Rev. Lett.* **28**, 1099 (1972). By coupling to the sample LC circuit directly in the helium bath we have obtained  $Q \approx 500$ , which is an order-of-magnitude improvement over commonly used circuits. A precision sample rotator provided the  $0.1^\circ$  reproducibility necessary in these experiments.

<sup>2</sup>J. M. Baker and J. P. Hurrell, *Proc. Phys. Soc., London* **82**, 742 (1963).

<sup>3</sup>U. Ranon and J. S. Hyde, *Phys. Rev.* **141**, 259 (1966).

<sup>4</sup>J. M. Baker, E. R. Davies, and J. P. Hurrell, *Proc. Roy. Soc., Ser. A* **308**, 403 (1968).

<sup>5</sup>D. Kiro and W. Low, in *Magnetic Resonance*, edited by C. K. Coogan, N. S. Ham, S. N. Stuart, J. R. Pilbrow, and G. V. H. Wilson (Plenum, New York, 1970).

<sup>6</sup>J. M. Baker and W. B. J. Blake, *Phys. Lett.* **31A**, 61 (1970).

<sup>7</sup>R. E. Watson and A. J. Freeman, *Phys. Rev. Lett.* **6**, 277 (1961).

<sup>8</sup>J. Kirton and S. D. McLaughlan, *Phys. Rev.* **155**, 279 (1967).